PHYSICAL REVIEW B **69**, 035201 (2004)

Electronic band structure of ordered vacancy defect chalcopyrite compounds with formula II-III$_2$-VI$_4$

Xiaoshu Jiang and Walter R. L. Lambrecht
Department of Physics, Case Western Reserve University, Cleveland, Ohio 44106-7079, USA

(Received 18 September 2003; published 13 January 2004)

First-principles local-density-functional calculations are presented for the electronic band structures of the ordered vacancy defect chalcopyrites with formula II-III$_2$-VI$_4$ for II = Zn, Cd, Hg, III = Al, Ga, In, and VI = S, Se, Te. Their relationship with the band structure of their parent chalcopyrite compounds I-III-VI$_2$ with I = Cu, Ag, and their grand parent II-VI compounds is clarified. An empirical correction for the band gaps beyond local-density approximation is introduced and shown to give good agreement for cases where data are available. The chemical trends are discussed.

DOI: 10.1103/PhysRevB.69.035201 PACS number(s): 71.20.Nr

I. INTRODUCTION

The chalcopyrite crystal structure is common to compounds of chemical formula II-IV-V$_2$ and I-III-VI$_2$. These can be thought of as being derived from a parent compound III-V and II-VI, respectively, by replacing the group-III element by alternating a group-II and group-IV element or the group II by a group-I and group-III element. Well-known examples are ZnGeP$_2$ and AgGaSe$_2$, respectively. All these compounds exhibit tetrahedral bonding and are derived from the zinc-blende crystal structure. The local valence is maintained as long as each group-V anion is surrounded by two group-II and two group-IV cations. The chalcopyrite structure corresponds to a particular ordering of the two types of cation.

Another class of tetrahedrally bonded materials, known as the defect chalcopyrites, exist and forms the subject of this paper. These can be considered ‘‘ordered vacancy’’ compounds. For example in a I-III-VI$_2$ compound, we may double the formula unit and then remove one of the group-I elements, thus creating a vacancy and replacing the other group I back by a group-II element to maintain the valency. For example CuGaSe$_2$ can be turned into Zn □ Ga$_2$Se$_4$, where □ represents the vacancy. Several of these compounds are known and a summary of their properties known so far can be found in Ref. 1. Different crystal structures with slightly different ordering of the cations and vacancies as well as order-disorder transitions exist in these materials. An excellent discussion of these issues can be found in Georgobiani *et al.*[2] and Bernard and Zunger.[3] In this paper we focus on the compounds which have the so-called thiogallate structure with space group $I\bar{4}$. Crystal structure data can also be found in Refs. 4–10. The knowledge about the band structure and optical properties of these compounds is still rather scarce. Optical absorption and band gaps were investigated in Refs. 11–14. Reflectivity spectra were measured for ZnGa$_2$Se$_4$ and CdGa$_2$S$_4$ by Turowski *et al.*[15] Some previous theory work can be found in Refs. 16, 17.

The reduction from cubic T_d symmetry of the zinc blende to tetragonal symmetry D_{2d} makes the chalcopyrite crystals birefringent and thus useful for nonlinear optical frequency conversion applications because the birefringence allows one to use angular tuning phase matching. Hence, some of the chalcopyrite semiconductors such as ZnGeP$_2$, CdGeAs$_2$, and AgGaSe$_2$ have found their primary applications in the development of optical parametric oscillators and frequency doublers in all solid-state tunable laser systems.[18] The even lower symmetry of the defect chalcopyrites S_4 suggests that they will be biaxial and may also have interesting nonlinear optical properties. Rather high nonlinear optical susceptibilities were measured by Levine *et al.* for CdGa$_2$S$_4$ and HgGa$_2$S$_4$ and explained on the basis of a bond-charge model.[13,14] The $\chi^{(2)}_{zxy}=2d_{36}$ was measured to be 27 pm/V for CdGa$_2$S$_4$, i.e., 20–30 % larger than AgGaS$_2$.[13] A similar value was measured for HgGa$_2$S$_4$ and the birefringence was found to be larger for this material.[14] While it is true that the lower symmetry will allow other nonzero components of the $\chi^{(2)}_{ijk}=2d_{ijk}$ tensor, the magnitude of the $\chi^{(2)}$ is known to vary strongly with band gap and the latter are still poorly known. In the point group $\bar{4}2m=D_{2d}$, the symmetry allowed components are $d_{14}\equiv d_{xyz}=d_{25}\equiv d_{yxz}$ and $d_{36}\equiv d_{zxy}$ which are further more equal in the static limit by Kleinman symmetry. In the pointgroup $\bar{4}=S_4$, the allowed components are all of the above and in addition: $d_{15}\equiv d_{xzx}=-d_{24}\equiv d_{yyz}$ and $d_{31}\equiv d_{zxx}=-d_{32}\equiv d_{zyy}$.

From an electronic structure theory point of view, the question arises how the band structures of these materials are related to those of their parent I-III-VI$_2$ compounds and the ‘‘grand parent’’ II-VI compounds. In this paper, we primarily investigate the band structure trends in this family of compounds and their relation to the parent compounds as a preliminary for future studies of the nonlinear optical properties.

II. COMPUTATIONAL METHOD

First-principles density-functional calculations are used in the local-density approximation (LDA).[19] The Hedin-Lundquist[20] parametrization is used for the exchange and correlation potential. The band structure method used is the linear muffin-tin orbital (LMTO) method in the atomic sphere approximation (ASA).[21] Brillouin zone integration is carried out with a regularly spaced mesh of $6\times6\times6$ points in the reciprocal unit cell and reduced by symmetry to 35 irreducible **k** points.

While in principle, we could optimize the lattice constants and internal structural parameters, we have here chosen to use experimental lattice constants as given in Refs. 1 and 4 and further explained in the following section. We have also investigated the effect of the atomic relaxations by comparing the band structures with idealized positions and experimental positions. Details are provided in the following section.

As is well known, the local-density approximation underestimates the band gap. However, in the present case, we can estimate corrections to the band gap based on the similarities of the band structure with the parent and grandparent compounds and using known results on the experimental band gaps of those.

As is also well known, the reason for the band gap underestimate in the LDA is that the Kohn-Sham one-particle equation strictly speaking does not provide quasiparticle excitation energies. The equation for quasiparticle energies in the so-called GW method,[22–25] differs from the Kohn-Sham equation by the fact that the local exchange-correlation potential v_{xc} is replaced by a nonlocal self-energy operator Σ_{xc} which is essentially the product of the one-electron Green's function G and the screened Coulomb interaction W. One of the major consequences of this is essentially a shift of the conduction-band states relative to the valence-band states. This effect can be simulated by shifting the diagonal elements of the LMTO Hamiltonian.

In the LMTO method the Hamiltonian has essentially a two-center tight-binding form:[21]

$$H_{RL,R'L'}(\mathbf{k})=C_{Rl}\delta_{RL,R'L'}+\sqrt{\Delta_{Rl}}S_{RL,R'L'}(\mathbf{k})\sqrt{\Delta_{R'l'}}, \tag{1}$$

in which $S_{RL,R'L'}(\mathbf{k})$ is the structure constant matrix, RL label the atomic sites R and angular momenta $L=lm$ of the basis set and C_{Rl} and Δ_{Rl} are potential parameters that determine, respectively, the "center of the Rl band" and the "width of the bands." To be precise, this Hamiltonian in the so-called nearly orthogonal representation is correct to second order in $(E-E_\nu)$ with E_ν the linearization energy of the LMTO method. In reality, we include further three-center correction terms and third-order corrections but these are irrelevant for the present purpose of explaining our gap correction method. The point is that by simply shifting the diagonal elements C_{Rl} we can modify the position of the center of the Rl band. It turns out that the conduction-band minimum at Γ in tetrahedrally bonded semiconductors has primarily cation s character, while the valence-band maximum has primarily anion p character. In the ASA, we introduce empty spheres at the tetrahedral interstices to fill space with spheres which are not too much overlapping. The wave functions then also contain expansions in muffin-tin orbitals centered at these empty sites. The s basis states on the empty sphere with nearest-neighbor cations also have a large contribution to the first few conduction-band states, and in particular strongly influence the position of the state at X. Since in chalcopyrite the states at X become folded at Γ, the first two conduction bands at X determine the position of the second and third conduction band at Γ for a direct-gap situation. Experience has shown that shifting of these empty sphere and cation s states by a few 0.1 Ry shifts the conduction bands up by the order of an eV without significantly modifying the valence bands. Thus we can semiempirically determine the necessary shifts to obtain a target band gap at X and Γ in II-VI compounds. In the process, the gaps at other $\mathbf{k}$ points also improve because they have a wave-function basis set composition intermediate between those states.

It is clear from a first-order perturbation theory point of view that these shifts essentially must correspond to the expectation values of $\Sigma_{xc}-v_{xc}$ and should therefore be representative of the particular LMTO basis state and be to some extent transferable from one compound to another. In order to make this approach useful for new compounds with as yet unknown band gaps, we need to show that the required shifts for II-VI compounds follow certain chemical trends and that similar shifts can then be applied to the I-III-VI$_2$ chalcopyrites and to the II-III$_2$-VI$_4$ defect chalcopyrites. We will in fact show that a universal shift essentially independent of cation provides already a basic improvement of all the gaps. Further details are provided in Sec. IV.

III. CRYSTAL STRUCTURE

The chalcopyrite crystal structure has a body-centered tetragonal Bravais lattice for which the primitive unit-cell lattice vectors can be chosen as $(a/2,a/2,-c/2)$, $(a/2,-a/2,c/2)$, $(-a/2,a/2,c/2)$. The unit-cell contains two formula units. The atomic positions are

$$\text{I:}\quad (0,0,0),(a/2,0,c/4)$$

$$\text{III:}\quad (a/2,a/2,0),(0,a/2,c/4)$$

$$\text{VI:}\quad (ua,a/4,c/8),(-ua,-a/4,c/8),(a/4,-ua,-c/8),$$
$$(-a/4,ua,-c/8).$$

In addition, in the ASA LMTO method, we place empty spheres at the positions

$$E_1:\quad (0,a/2,0),(a/2,0,0)$$

$$E_2:\quad (a/4,-a/4,c/8),(-a/4,a/4,c/8),(a/4,a/4,-c/8),$$
$$(-a/4,-a/4,-c/8)$$

$$E_3:\quad (0,0,c/4),(a/2,a/2,c/4).$$

The ratio $\eta=c/2a$ is 1 for the idealized structure and the parameter $u=1/4$ for the idealized structure. In most cases, $\eta<1$ and $u>1/4$ which implies that III-VI bond length is shorter than the I-VI bond length.

In the defect chalcopyrite structure, the second of the group-I elements is missing and replaced by an empty sphere of type E_4. Furthermore, the position of the anion VI now can deviate from the ideal 1/4 position in all three directions. So, there are now three internal structural parameters (x,y,z). Some caution must be used in using the crystallographic data given in Ref. 1. The atomic positions in Ref. 1 are

$$vacancy: \quad (0,0,0)$$

$$\text{I:} \quad (0,1/2,1/4)$$

$$\text{III:} \quad (0,0,1/2),(1/2,0,1/4),$$

$$\text{VI:} \quad (x,y,z),(-x,-y,z),(-y,x,-z),(y,-x,-z),$$

in units of a for x and y coordinates and in units of c for the z coordinate. Most values given in the table for x, y, and z are such that the atoms would seem to move away from the vacancy and toward the group-II atom. This seems unlikely. It turns out that the original paper by Hahn *et al.*[4] gives the same x, y, z values but places the group-II atom at the origin. The atomic positions given in Ref. 4 are

$$\text{II:} \quad (0,0,0)$$

$$\text{III:} \quad (0,0,1/2),(0,1/2,1/4)$$

$$\text{VI:} \quad (x,y,z),(-x,-y,z),(x,-y,-z),(-x,y,-z).$$

These present another problem. Apparently the symmetry is wrong here. For defect chalcopyrite compounds II-III$_2$-VI$_4$, the S_4 rotation reflection operation requires

$$\text{VI:} \quad (x,y,z),(-x,-y,z),(y,-x,-z),(-y,x,-z).$$

Reference 1 corrected the symmetry problem but erroneously put the vacancy in the origin instead of the group-II cation and it also interchanged the positions of vacancy and group III, which lead to a wrong crystal structure.

We adopt the crystal structure of the defect chalcopyrite as follows:

$$\text{II:} \quad (0,0,0)$$

$$\text{III:} \quad (0,0,1/2),(0,1/2,1/4)$$

$$\text{VI:} \quad (x,y,z),(-x,-y,z),(y,-x,-z),(-y,x,-z).$$

We note that in this crystal structure there are two inequivalent III-VI bond lengths and chemically inequivalent group-III atoms. Thus, the conservation of tetrahedral bond lengths model of Bernard and Zunger[3] cannot be used to estimate the internal coordinates. The defect chalcopyrite structure is illustrated in Fig. 1.

IV. RESULTS

We start by discussing the relation between the band structures of the defect chalcopyrite compound and its parent and grand parent compounds.

As an example, we show the band structures of ZnSe, CuGaSe$_2$, and ZnGa$_2$Se$_4$ all displayed in the same chalcopyrite structure Brillouin zone. The Brillouin zone is shown in Fig. 2. This case is chosen because the chemical substitutions all happen within the same row of the periodic table. We find that the gap decreases strongly from ZnSe to CuGaSe$_2$ and then increases again going to ZnGa$_2$Se$_4$. This can be explained mainly in terms of the behavior of the d orbitals. The Zn $3d$ bands lie at about -9.5 eV, i.e., below the Se $4p$ valence band. The Cu $3d$ bands lie higher in energy and strongly hybridize with the Se $4p$ bands, in fact creating a second gap within the valence band (Figs. 3 and 4). The conduction-band minimum is mostly Ga $4s$ rather than Cu $4s$ like. When Cu is replaced again by Zn, the band gap reopens and in fact the final band gap is larger than that of ZnSe itself.

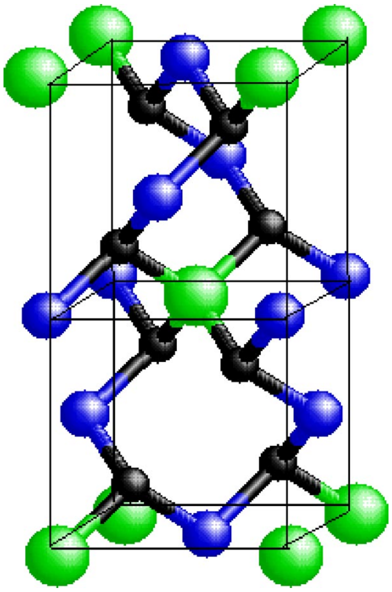

FIG. 1. (Color online) Defect chalcopyrite crystal structure.

The band structures for other compounds are similar in overall appearance. The band gaps are summarized in Table III.

So far, we have only shown the LDA band structures. To correct the band gaps, we first considered what shifts need to

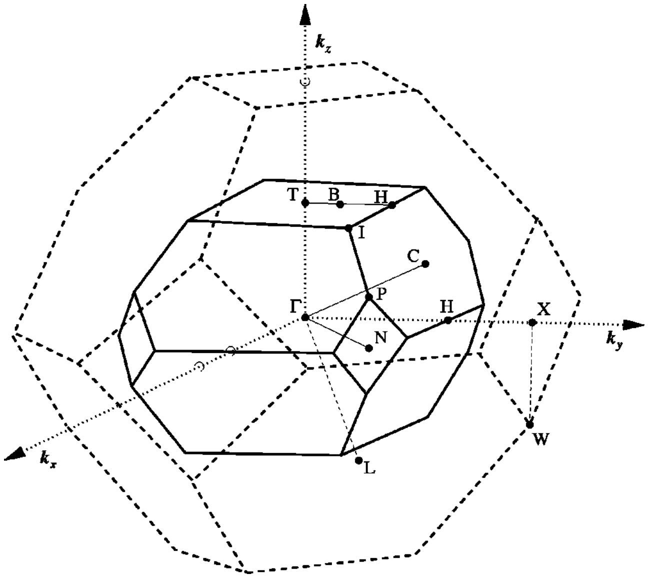

FIG. 2. First Brillouin zone (BZ) of chalcopyrite structure (solid lines) and its relation to that of the zinc-blende (ZB) structure (dashed lines). The points X, L, and W lie on the ZB BZ.

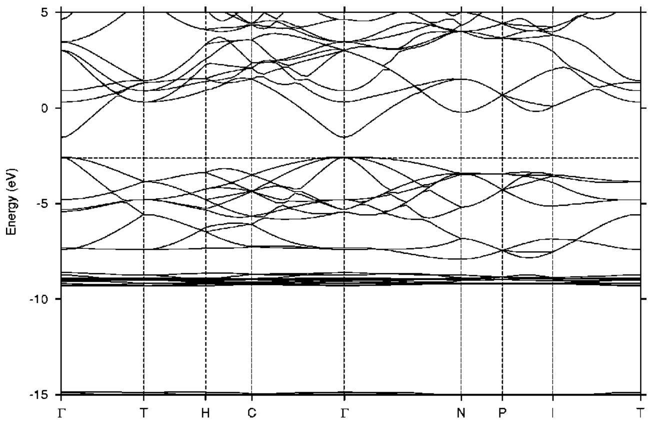

FIG. 3. Band structure of ZnSe in chalcopyrite Brillouin zone.

TABLE I. Band gaps in II-VI compounds with and without corrections. All values in eV.

Compound	LDA		Corrected		GW[a]	
	Γ	*X*	Γ	*X*	Γ	*X*
CdS	1.04	5.33	2.84	6.54	2.83	6.82
CdSe	0.47	4.94	2.35	6.17	2.01	6.15
CdTe	0.47	4.42	1.76	5.21	1.76	5.14
ZnS	1.89	5.51	3.56	6.71	3.98	7.20
ZnSe	1.01	5.10	2.86	6.32	2.84	6.49
ZnTe	0.85	4.52	2.11	5.08	2.57	5.63

[a] Reference 26.

be applied to the group-II *s* like states and empty sphere *s* states in the II-VI's. For simplicity, we decided to try to introduce as few parameters as possible. We adjust the shifts so as to reproduce the *GW* results of Zakharov *et al.*[26] rather than experimental results because we wish to adjust not only the minimum gap but both gaps at Γ and *X*. We find that we can obtain fairly good agreement applying the same shift of 0.21 Ry for the Zn, Cd, and Hg *s* states and the same shifts apply to S and Se compounds, but a slightly lower shift of 0.14 Ry must be applied to the Te compounds. A shift of the cation surrounded empty sphere *s* level is needed to adjust the *X* point band gap. We find that we can use the same value as for the cation *s* shift, i.e., 0.21 Ry and 0.14 Ry, respectively, for (S, Se) and Te compounds. The corrections of the band gaps at Γ and *X* obtained using these shifts are given in Table I. Of course, one could fine tune the shifts for each compound. However, the main point we see here is that the shifts are almost universal. Thus, we can apply the same shifts to the cations in I-III-VI$_2$ and II-III$_2$-VI$_4$ compounds.

Inspection of the eigenvectors of the conduction-band minimum in I-III-VI$_2$ and II-III$_2$-VI$_4$ compounds shows that the contribution of I*s*, II*s* and III*s* orbitals is in fact comparable in magnitude with a slightly larger group-III component. We shift both the I*s* and III*s* levels in I-III-VI$_2$ chalcopyrites and II*s* and III*s* levels in II-III$_2$-VI$_4$ defect chalcopyrites. The comparison with experimental data for the I-III-VI$_2$ compounds is shown in Table II and is satisfactory considering we only used two parameters. Note that in several cases LDA gives the wrong trends for Se and Te compounds, and after the shift, all of them have the same trends as experimental data suggested. The results are represented graphically in Fig. 5.

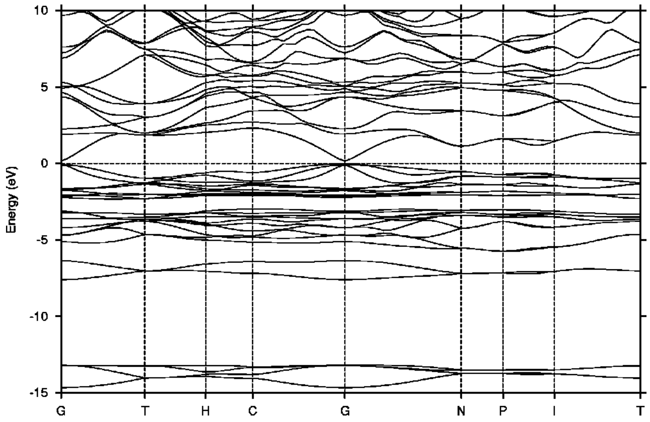

FIG. 4. Band structure of CuGaSe$_2$.

From Fig. 6 and Table III we can see that for all cases where experimental value are available for the defect chalcopyrites, the agreement between theory and experiment becomes rather good after this correction is applied. We thus can consider the other cases as predictions.

Next, we consider the effects of the deviations of the internal parameters from their ideal positions. The LDA gaps for ideal and experimental atomic positions are listed in Table III. We compare the LDA results for the ideal and experimental parameters. First, for nine of them, they are the same and thus have the same LDA gaps. However, closer

TABLE II. Energy gaps of chalcopyrites.

Compound	LDA	Corrected	Experiment[a]
CuAl$_2$S$_4$	1.50	3.00	3.49–3.62
CuAl$_2$Se$_4$	0.80	2.49	2.65–3.02
CuAl$_2$Te$_4$	1.20	2.22	2.06
CuGa$_2$S$_4$	0.85	2.42	2.43–2.65
CuGa$_2$Se$_4$	0.14	1.77	1.68–2.01
CuGa$_2$Te$_4$	0.35	1.41	1–1.24
CuIn$_2$S$_4$	0.19	1.77	1.53–1.62
CuIn$_2$Se$_4$	0.01	1.35	1.04–1.27
CuIn$_2$Te$_4$	0.41	1.42	1.06–1.67
CuTl$_2$S$_4$	0.02	1.58	
CuTl$_2$Se$_4$	0.02	1.19	
AgAl$_2$S$_4$	1.05	2.66	
AgAl$_2$Se$_4$	0.48	2.16	
AgAl$_2$Te$_4$	0.68	1.80	2.27
AgGa$_2$S$_4$	0.82	2.40	2.64–3.01
AgGa$_2$Se$_4$	0.19	1.42	1.80–2.28
AgGa$_2$Te$_4$	0.04	1.08	1.32
AgIn$_2$S$_4$	0.34	1.99	1.87–2.06
AgIn$_2$Se$_4$	0.10	1.60	1.24–1.6
AgIn$_2$Te$_4$	0.14	1.25	0.95–1.12

[a] Reference 1.

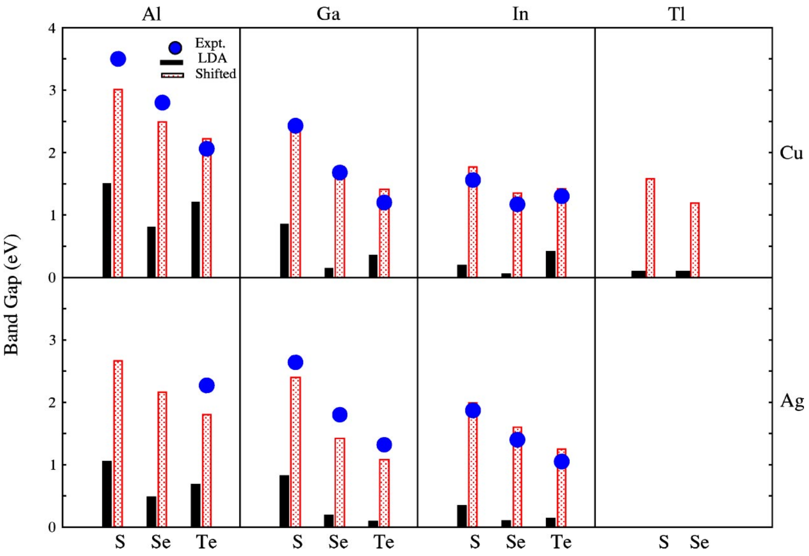

FIG. 5. (Color online) Band gaps of chalcopyrites.

inspection of the experimental work[4] reveals that in most of these cases, the space group of the system is actually uncertain. It could be either $I\bar{4}$ or $I\bar{4}2m$. Thus the structural parameters x,y,z were not really obtained by refining the agreement between measured and calculated structure factors. In the other cases, using the experimental parameters can either raise or lower the band gaps. Experimental data on the gaps are only available for a few cases and we shall examine those in more detail. Looking into the Table III, we can see that there are three compounds ($ZnIn_2Se_4$, $CdGa_2Te_4$, $CdIn_2Te_4$) which have slightly larger differences between the calculated and experimental gaps than others. We believe the discrepancy may be caused by the inaccuracy in the measured atomic positions. For $ZnIn_2Se_4$, the LDA (ideal) gives 1.33 eV gap, which is larger than the LDA gap 1.05 eV using experimental positions. Our corrected result has a larger gap 2.33 eV (compared to the $\sim$2 eV experimental value). Since the relaxation from ideal positions makes the LDA gap smaller, which usually translates into a smaller energy gap after being shifted, we would anticipate fully relaxed parameters could give a better fit if the actual relaxed positions are further away from the ideal positions than indicated by the experimental structure determination. In $CdIn_2Te_4$, the relaxation lowers the LDA gap from 1.03 eV to 0.96 eV. Again, our calculated gap 1.80 eV$>$1.25 eV (experimental gap). Thus, a stronger relaxation might improve the agreement. However that could not explain the trend in $CdGa_2Te_4$, where further relaxation will only make the calculated gap worse. But the only two experimental gaps we get from MacKinnon *et al.*[1] are 1.4 eV for disordered zinc blende and 1.5 eV for an uncertain structure (body-centered-tetragonal structure or $I\bar{4}$), so we will put this one aside until further experimental data are available.

The discrepancies of I-III-VI_2 chalcopyrites could also be partly due to inaccurate atomic positions. Another possible reason could of course be that we need more parameters to fine tune the gap shifts. However, if we need too many parameters then the model loses its purpose. For our current purposes of understanding the gap trends and obtaining a reasonable agreement with experiments throughout the family of compounds, the model with only two parameters seems sufficient. We believe fully optimized atomic positions

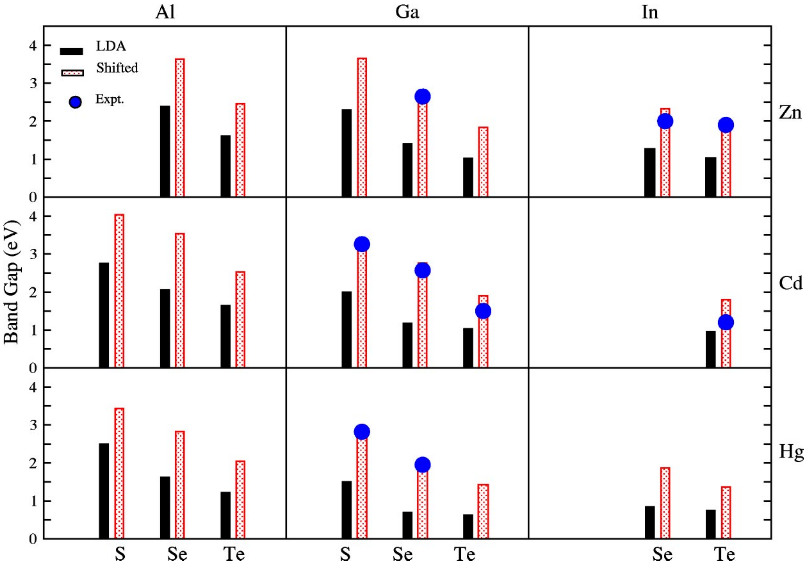

FIG. 6. (Color online) Band gaps of defect chalcopyrites.

TABLE III. Energy gaps of some defect chalcopyrites.

Compound	LDA(ideal)	LDA	Corrected	Experiment [a]	Other calculations
$ZnAl_2Se_4$	2.17	2.23	3.65		
$ZnAl_2Te_4$	1.61	1.61	2.46		
$ZnGa_2S_4$	2.29	2.29	3.65		3.6 [b]
$ZnGa_2Se_4$	1.40	1.40	2.73	2.58–2.71 [c]	
$ZnGa_2Te_4$	1.02	1.02	1.84		
$ZnIn_2Se_4$	1.33	1.05	2.33	2.0–2.05	
$ZnIn_2Te_4$	1.03	1.03	1.90	1.87–1.90	
$CdAl_2S_4$	2.59	2.61	4.04		
$CdAl_2Se_4$	1.92	2.13	3.54		
$CdAl_2Te_4$	1.64	1.64	2.53		
$CdGa_2S_4$	1.79	1.99	3.30	3.25–3.44	
$CdGa_2Se_4$	1.27	1.42	2.76	2.57	
$CdGa_2Te_4$	0.94	1.08	1.90	1.5	
$CdIn_2Te_4$	1.03	0.96	1.80	1.25	
$HgAl_2S_4$	2.27	2.18	3.43		2.54 [d]
$HgAl_2Se_4$	1.51	1.57	2.83		
$HgAl_2Te_4$	1.22	1.22	2.04		
$HgGa_2S_4$	1.44	1.57	2.86	2.79–2.84	
$HgGa_2Se_4$	0.69	0.69	1.92	1.95	1.66 [b]
$HgGa_2Te_4$	0.63	0.63	1.43		
$HgIn_2Se_4$	0.80	0.63	1.87		
$HgIn_2Te_4$	0.68	0.59	1.37		

[a] Reference 1.
[b] Reference 16.
[c] Reference 15.
[d] Reference 17.

would improve the overall fitting in both chalcopyrites and defect chalcopyrites and it will be included in our further work on this subject.

We note that we find all the band gaps of the II-III_2-VI_4 compounds to be direct. In most of these compounds, the nature of the band gap has been under discussion. For instance, in $CdGa_2S_4$, an indirect gap of 3.05 eV was reported by Radautsan *et al.*,[27] while a direct gap of 3.44 eV was reported by Kshirsagar and Sinha[28] both based on absorption measurements. Our result 3.30 eV and the band structure both support the direct gap. Further experimental results based on other measurement techniques can be found in MacKinnon *et al.*[1] In $CdGa_2Se_4$, the size and nature of the electronic energy gap are not clear. They range from an indirect gap of 1.97 eV to a direct gap of 2.57 eV or higher. Our calculations give a direct gap of 2.76 eV. For $ZnIn_2Te_4$, there were some reports of indirect gap about 1.4 eV.[29,30] We have an energy gap of about 1.9 eV, which agrees well with the experimental direct gap (1.9 eV). For $ZnGa_2Se_4$, reflectivity spectra were reported by Turowski *et al.*[15] Our minimum gap is in fair agreement with their assignment of the E_1 feature as a direct-gap transition. However, their spectrum also indicates a lower-energy feature D at 1.98 eV which is presumably due to defects. Mostly, the suggestions of indirect gaps are based on the observation of weak absorption band tails. Our results strongly suggest that alternative explanations in terms of defects or disorder must be invoked to explain these absorption tails.

Finally, we examine the chemical trends of the band gaps. Clearly, since the gap shifts are not very material dependent, these trends are already clear from the LDA gaps. We clearly see a decrease in gap from Al to Ga to In and from S to Se to Te. There is also a less pronounced trend of decrease of the gaps from Zn to Cd to Hg. These are the expected trends. For heavier elements the cation s states become deeper because the s states are nonzero at the origin and thus feel the nuclear potential and hence decrease with Z. The conduction-band minimum has typically a slightly larger group IIIs than IIs contribution, thus explaining why the trend with the III element is more pronounced. The decrease in gap from S to Se to Te on the other hand is related to the strength of the bonding. We may see that along this series the gap opens across the entire BZ rather than just near the minimum gap at Γ. To illustrate this point we show the band structures of $CdGa_2S_4$, $CdGa_2Se_4$, and $CdGa_2Te_4$ in Figs. 7, 8, and 9. On the other hand, the band structures of the series $ZnAl_2Se_4$, $ZnGa_2Se_4$, $ZnIn_2Se_4$ shown in Figs. 10, 11, 12 illustrates how the change of the III element affects the band structure while keeping the anion and II element fixed. In the former series we see an overall change of the band gap throughout the Brillouin zone while in the latter, the gap is mostly affected near Γ. Finally, the band structures in the series

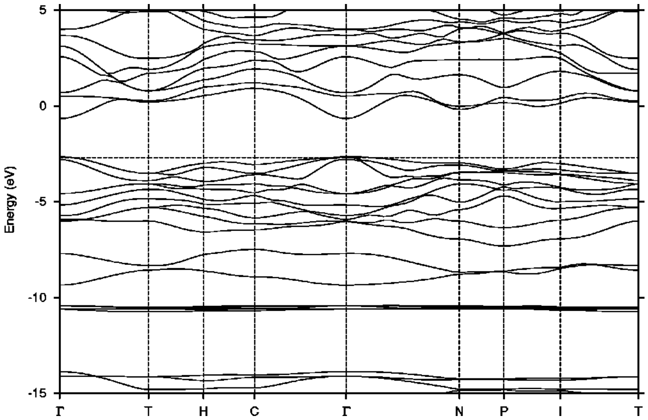

FIG. 7. Band structure of $CdGa_2S_4$.

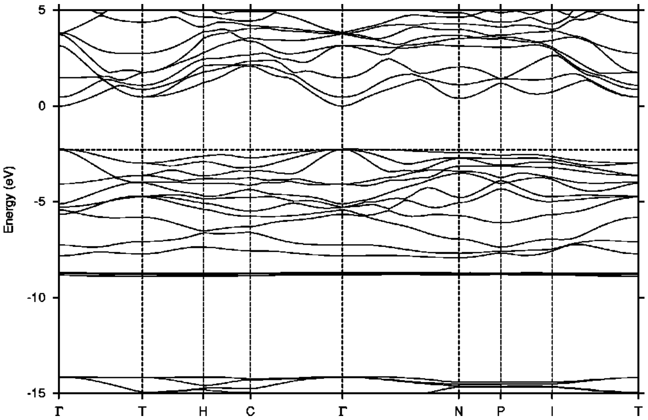

FIG. 10. Band structure of $ZnAl_2Se_4$.

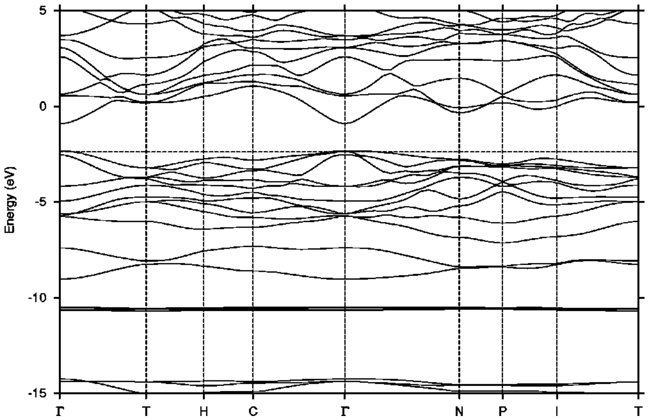

FIG. 8. Band structure of $CdGa_2Se_4$.

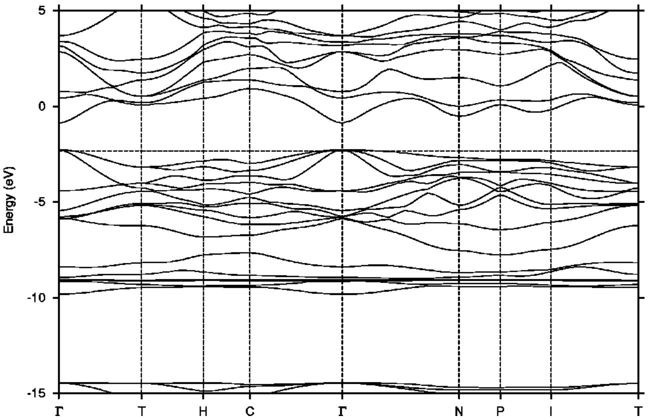

FIG. 11. Band structure of $ZnGa_2Se_4$.

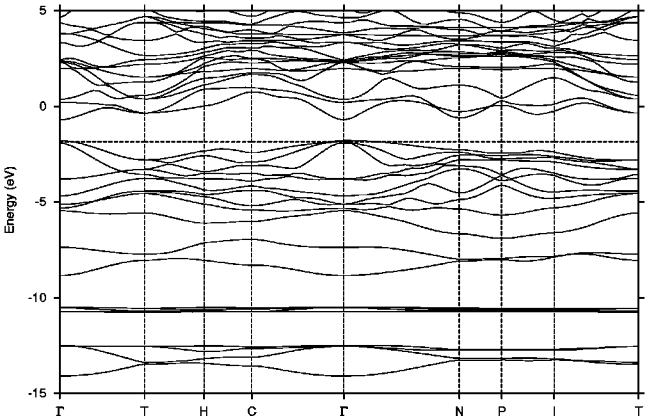

FIG. 9. Band structure of $CdGa_2Te_4$.

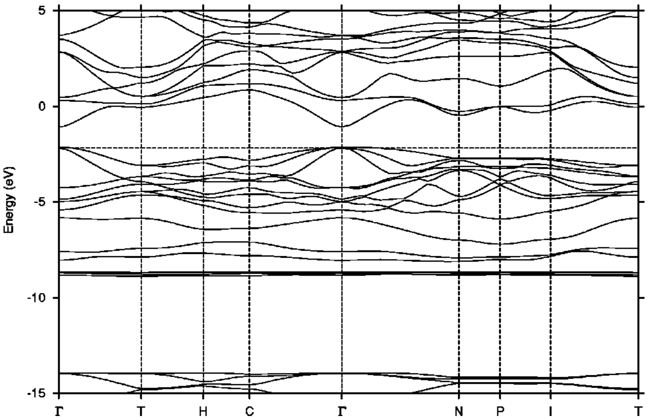

FIG. 12. Band structure of $ZnIn_2Se_4$.

$ZnGa_2Se_4$, $CdGa_2Se_4$, $HgGa_2Se_4$. Figures 11, 8, and 13 illustrate that the trend with group-II element is similar to that of the group-III element but less pronounced.

V. CONCLUSION

In this paper, we have investigated the band structure and band gaps of a family of compounds known as the defect chalcopyrites or thiogallates. Using a simple empirical band-gap correction with a minimal number of parameters (in fact only two) we obtained satisfactory agreement with experiment for all grandparent II-VI, parent I-III-VI_2, and for those defect chalcopyrites for which experimental data are available. We have clarified that all band gaps are direct and in this family and have explained the trends in the band gaps.

From the point of view of nonlinear optical applications, we note that the larger band gaps than in the I-III-VI_2 chalcopyrites will usually tend to lead to smaller $\chi^{(2)}$. However, such a rule only applies within a given family of materials. We note that compared to I-III-VI_2 compounds, the corresponding II-VI compounds have larger $\chi^{(2)}$. Thus, one may perhaps also expect that II-III_2-VI_4 compounds will also have larger $\chi^{(2)}$ as is borne out by Levine's measurements and explained within his bond charge model.[13,14] On the other hand, the direct nature of these materials may also open the way to other optoelectronic applications, in particular for the wide band-gap materials in the family.

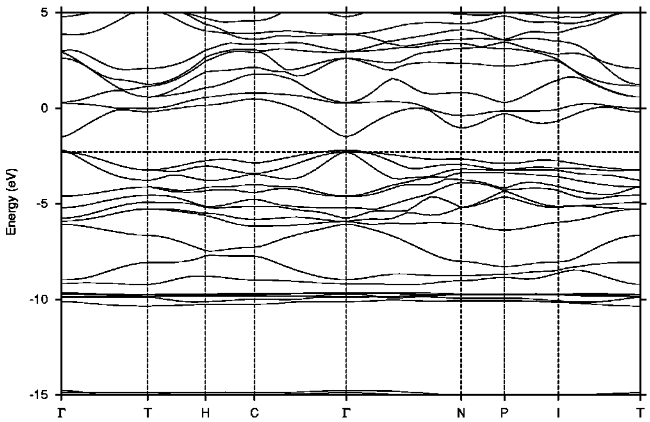

FIG. 13. Band structure of $HgGa_2Se_4$.

ACKNOWLEDGMENTS

This work was supported by the Air Force Office of Scientific Research under Grants Nos. F49320-00-1-0037 and F49620-03-1-0010.

---

[1] MacKinnon, in *Tables of Numerical Data and Funtional Relationships in Science and Technology*, edited by O. Madelung, Landolt-Börnstein New Series, Group III, Vol. 17, pt. h (Springer-Verlag, Berlin, 1985), p. 124.

[2] A.N. Georgobiani, S.I. Radautsan, and I.M. Tiginyanu, Fiz. Tekh. Poluprovodn. **19**, 193 (1985) [Sov. Phys. Semicond. **19**, 121 (1985)].

[3] J.E. Bernard and A. Zunger, Phys. Rev. B **37**, 6835 (1988).

[4] H. Hahn, G. Frank, W. Klinger, A.D. Störger, and G. Störger, Z. Anorg. Allg. Chem. **279**, 241 (1955).

[5] H. Hahn and W. Klingler, Z. Anorg. Allg. Chem. **263**, 177 (1950).

[6] H. Schwer and V. Krämer, Z. Kristallogr. **190**, 102 (1990).

[7] V. Krämer, B. Frick, and D. Siebert, Z. Kristallogr. **165**, 151 (1983).

[8] V. Krämer, H. Hirth, W. Hofherr, and H.-P. Trah, Thermochim. Acta **112**, 89 (1987).

[9] S.I. Radautsan, F.G. Donika, G.A. Kyosse, and I.G. Mustya, Phys. Status Solidi A **37**, K123 (1970).

[10] H.J. Berthold, K. Köhler, and R. Wartchow, Z. Anorg. Allg. Chem. **496**, 7 (1983).

[11] J.A. Beun, R. Nitsche, and M. Lichtensteiger, Physica (Amsterdam) **27**, 448 (1961).

[12] H. Haeuseler, J. Solid State Chem. **26**, 367 (1978).

[13] B.F. Levine, C.G. Bethea, and H.M. Kasper, IEEE J. Quantum Electron. **QE-10**, 904 (1974).

[14] B.F. Levine, C.G. Betha, H.M. Kasper, and F.A. Thiel, IEEE J. Quantum Electron. **QE-10**, 904 (1974).

[15] M. Turowski, A. Kisiel, and W. Giriat, J. Phys. C **17**, L661 (1984).

[16] V.L. Panyutin, B.E. Ponedel'nikov, A.E. Rozenson, and V.I. Chizhkov, Fiz. Tekh. Poluprovodn. **13**, 1211 (1979) [Sov. Phys. Semicond. **13**, 857 (1979)].

[17] V.L. Panyutin, B.E. Ponedel'nikov, A.E. Rozenson, and V.I. Chizhkov, Fiz. Tekh. Poluprovodn. **14**, 1230 (1980) [Sov. Phys. Semicond. **14**, 728 (1980)].

[18] M.C. Ohmer and R. Pandy, MRS Bull. **23**, 16 (1998).

[19] W. Kohn and L.J. Sham, Phys. Rev. **140**, A1133 (1965).

[20] L. Hedin and B.I. Lundqvist, J. Phys. C **4**, 2064 (1971).

[21] O.K. Andersen, Phys. Rev. B **12**, 3060 (1975); O. K. Andersen, O. Jepsen, and M. Šob, in *Electronic Band Structure and its Applications*, edited by M. Yussouf (Springer, Heidelberg, 1987), p. 1.

[22] L. Hedin and S. Lundqvist, in *Solid State Physics, Advances in Research and Applications*, edited by F. Seitz, D. Turnbull, and H. Ehrenriech, (Academic Press, New York 1969), Vol. 23, p. 1.

[23] M.S. Hybertsen and S.G. Louie, Phys. Rev. Lett. **55**, 1418 (1985); Phys. Rev. B **34**, 5390 (1986).

[24] R.W. Godby, M. Schlüter, and L.J. Sham, Phys. Rev. Lett. **56**, 2415 (1986); Phys. Rev. B **37**, 10 159 (1988).

[25] F. Aryasetiawan and O. Gunnarsson, Rep. Prog. Phys. **61**, 237 (1998).

[26] O. Zakharov, A. Rubio, X. Blase, M.L. Cohen, and S.G. Louie, Phys. Rev. B **50**, 10 780 (1994).

[27] S.I. Radautsan, N.N. Syrba, I.I. Nebola, V.G. Tyrziu, and D.M. Bercha, Fiz. Tekh. Poluprovodn. **11**, 69 (1977) [Sov. Phys. Semicond. **11**, 38 (1977)].

[28] S.T. Kshirsagar and A.P.B. Sinha, J. Mater. Sci. **12**, 1614 (1977).

[29] P. Manca, F. Raga, and A. Spiga Phys. Status Solidi A **16**, K105 (1973).

[30] P. Manca, F. Raga, and A. Spiga, Ind. Eng. Chem. **19**, 15 (1974).